AIAA JOURNAL
Vol. 39, No. 11, November 2001

# Optimized Nonuniform Rational B-Spline Geometrical Representation for Aerodynamic Design of Wings

Jérôme Lépine,* François Guibault,† and Jean-Yves Trépanier‡
*École Polytechnique de Montréal, Montréal, Québec H3T 1J4, Canada*
and
François Pépin§
*Bombardier Aerospace, Dorval, Québec H4S 1Y9, Canada*

**The geometric representation and parameterization used in an aerodynamic wing design process determines the number of design variables and influences the smoothness of the wing representation. In an attempt to reduce the number of design variables while preserving good smoothness properties, the present research investigates the performance of an optimized nonuniform rational B-spline (NURBS) geometrical representation for the aerodynamic design of wings. As a first step, an approach is described whereby optimal spatial positions and weights of a fixed number of NURBS control points is determined using a quasi-Newton optimization algorithm to approximate a general airfoil section. The resulting optimized NURBS representation significantly reduces the number of design variables needed to define accurately a wing section while ensuring good smoothness properties. In a second step, the NURBS control point positions and weights are used as design variables in an aerodynamic optimization problem. This methodology results in a rapid and robust design process, as illustrated by examples of aerodynamic optimization for two- and three-dimensional cases.**

## Nomenclature

| | | |
|---|---|---|
| $\boldsymbol{A}(u)$ | = | position of point on nonuniform rational B-spline (NURBS) curve |
| $C_p$ | = | local pressure coefficient |
| $d_j$ | = | local distance between approximation and target |
| $F(\boldsymbol{X})$ | = | objective function |
| $\boldsymbol{H}$ | = | approximated Hessian matrix of $F$ |
| $M$ | = | Mach number |
| $m$ | = | number of points used for computing approximation error |
| $N_{i,p}$ | = | NURBS interpolation function (order $p$) |
| $n$ | = | number of NURBS control points |
| $P_i$ | = | NURBS control point position |
| $R_{i,p}$ | = | NURBS interpolation function of order $p$ |
| $\boldsymbol{S}$ | = | descent direction vector |
| $u$ | = | parameter defining NURBS curve |
| $\boldsymbol{X}$ | = | vector of design parameters |
| $x, y, z$ | = | Cartesian body axes |
| $\alpha$ | = | line-search step size |
| $\varepsilon_{\max}$ | = | maximal approximation error |
| $\varepsilon_{\text{mea}}$ | = | average approximation error |
| $\omega$ | = | weights of NURBS control points |

## I. Introduction

GEOMETRICAL representation and parameterization are crucial issues, the importance of which has often been underestimated in wing design processes. However, with the renewed interest in optimization, in particular in the context of multidisciplinary design and optimization (MDO), researchers are revisiting the problem to find efficient and robust parameterizations of the surfaces. In a recent paper, Samareh[1] identifies three categories of approach to geometrical representation in the context of aerodynamic and MDO. These are the discrete approach, the CAD approach, and the free-form deformation approach, each with its own benefits and drawbacks. In the present paper, nonuniform rational B-splines (NURBS) are used for geometrical representations of airfoil shapes, and so this method falls into the CAD-based approach category.

In selecting a geometrical representation and parameterization for aerodynamic design, a first issue is to reduce the resulting number of design variables as much as possible while maintaining sufficient freedom and flexibility to represent a large class of airfoil sections. In fact, in a design optimization process, the geometrical definition of the wing section, and of the wing, can be directly linked to the number of design variables. A method that reduces the number of parameters involved in the geometric representation of a two-dimensional airfoil profile can simplify the design process. Furthermore, the ability of the geometrical representation to filter a nonrealistic airfoil (i.e., to ensure good surface smoothness properties) is a second issue that will in many ways help an aerodynamic optimization process converge to realistic shapes.

In the present paper, the efficiency of NURBS will be investigated systematically for the geometric representation of airfoil sections and for their aerodynamic optimization. A methodology developed for the approximation of a given airfoil section will provide an initial guess for the aerodynamic design optimization. This initial approximation is obtained by solving a purely geometric optimization problem where the objective function measures the error of the representation. The result of this first optimization is a reduction in the number of design variables required to represent an airfoil.

The aerodynamic optimization problem then uses the NURBS control point positions and weights as design variables in an optimization problem where the objective is to minimize the difference between the airfoil pressure distribution and a prescribed pressure distribution.

The paper is organized as follows: In the following section, the methodology used to approximate a given airfoil with an optimized NURBS curve is detailed. In Sec. III, results are presented that demonstrate the efficiency of the approximation method in reducing the number of design parameters while ensuring the smoothness of the airfoil representation. Then, in Sec. IV the optimized NURBS representations are used to perform aerodynamic optimizations of airfoils and wings. The results illustrate the robustness and efficiency of the method for wing design.

Received 2 July 2000; revision received 28 November 2000; accepted for publication 10 April 2001. Copyright © 2001 by the American Institute of Aeronautics and Astronautics, Inc. All rights reserved.

*M.S. Student, Department of Mechanical Engineering.
†Assistant Professor, Department of Electrical and Computer Engineering; also Member, Centre de Recherche en Calcul Appliqué, 5160 Boul. Décarie, Suite 400, Montréal, QC H3X 2H9, Canada.
‡Associate Professor, Department of Mechanical Engineering; also Member, Centre de Recherche en Calcul Appliqué, 5160 Boul. Décarie, Suite 400, Montréal, QC H3X 2H9, Canada. Senior Member AIAA.
§Aerodynamic Design Engineer, Advanced Aerodynamics Department.

## II. Approximation Problem

A NURBS curve is defined such that

$$\boldsymbol{A}(u) = \sum_{i=0}^{n} R_{i,p}(u)\boldsymbol{P}_i \tag{1}$$

with

$$R_{i,p}(u) = \frac{N_{i,p}(u)\omega_i}{\sum_{j=0}^{n} N_{j,p}(u)\omega_j} \tag{2}$$

where $\boldsymbol{P}_i$ are the control point coordinates, $\omega_i$ their respective weights, $N_{i,p}$ the $p$th-degree B-spline basis functions, and $\boldsymbol{A}(u)$ the position of a point on the curve. The basis functions are obtained through a knot vector, which defines the functions' break points, of the form

$$\{\underbrace{0, \ldots, 0}_{p+1}, u_{p+1}, \ldots, u_{m-p+1}, \underbrace{1, \ldots, 1}_{p+1}\}$$

NURBS are fully described in Ref. 2.

### A. Approximation Error

With these interpolation functions, the problem of approximating a general planar curve $\mathcal{C}(t)$ can be stated as follows: Find the set of control points $\boldsymbol{P}_i$ and weights $\omega_i$ such that $\|\boldsymbol{A}(u) - \mathcal{C}(t)\|$ is minimized in a suitable norm.

Theoretically, the $L_2$ norm would be a natural choice; numerically, though, for a completely general target curve, this norm can only be approximated through discretization. Numerical experiments have, thus, been carried out to develop and validate a robust computational approach for the determination of the approximation error. Consideration has been given to both the mean and the maximum error, as well as to the level of continuity of the target curve. Three classes of target curve have been considered: curves only given as a set of points, piecewise linear curves, and $C^1$ or more continuous curves. In all cases, the mean error $\varepsilon_{\text{mea}}$ is determined by summing the distance $d_j$ of a set of points chosen on the target curve to their respective projections on the approximation curve and the maximum error $\varepsilon_{\max}$ by determining the largest of these distances. We thus have

$$\varepsilon_{\text{mea}} = \frac{1}{n}\sum_{j=1}^{n} d_j \tag{3}$$

$$\varepsilon_{\max} = \max_{1 \le j \le n} d_j \tag{4}$$

In light of these experiments, it was determined that the error computed using the control points constitutes an adequate bound on both the mean and the maximum error of approximation, and this error can be computed at a fraction of the cost of using evenly spaced discretization points. This method of computing the error also has the property of naturally including the case of target curves given as a discrete set of points, which is not a rare case in many practical applications. Details concerning the evaluation of norms can be found in Ref. 3.

### B. Optimization Method

With these definitions and this computational method of error approximation, the optimization problem can be further specified by introducing a cost function of the form

$$F(\boldsymbol{X}) = 2 \times \varepsilon_{\text{mea}} + \varepsilon_{\max}$$

where $\boldsymbol{X}$ is the vector of design variables, in this case the positions and weights of the control points of the approximation curve: $\boldsymbol{X} = \{x_1, y_1, \omega_1, x_2, \ldots, x_n, y_n, \omega_n\}$. This choice of a cost function accelerates convergence of the optimization process by including both the maximum error, which controls the quality of the final approximation, and the mean error, which globally compares the quality of different solutions.

Clearly, this is a nonlinear optimization problem, and we will now examine the solution process chosen, including the choice of an initial solution.

### C. Solution Method

The primary solution method used was the second-order quasi-Newton method, which, given a reasonably close initial solution $\boldsymbol{X}_0$, will iteratively converge toward an optimal solution using the relation

$$\boldsymbol{X}_{k+1} = \boldsymbol{X}_k + \alpha_k \boldsymbol{S}_k$$

where $\boldsymbol{S}_k = -\boldsymbol{H}_k \cdot \nabla F(\boldsymbol{X}_k)$ is the direction of descent vector and $\alpha_k$ the distance of descent in direction $\boldsymbol{S}_k$. The descent vector is computed using the Broyden–Fletcher–Goldfarb–Shanno (BFGS) algorithm, based on a second-order approximation of the gradient of $F(\boldsymbol{X})$:

$$\nabla F(\boldsymbol{X}) \simeq \nabla F(\boldsymbol{X}_k) + \boldsymbol{H}(\boldsymbol{X}_k) \cdot \delta\boldsymbol{X}$$

where $\delta\boldsymbol{X} = \boldsymbol{X} - \boldsymbol{X}_k$ is used as the direction of the descent vector $\boldsymbol{S}_k$. Here, $\boldsymbol{H}$, the approximate Hessian matrix, is initially set to identity and iteratively updated using the relation

$$\boldsymbol{H}_{k+1} = \boldsymbol{H}_k + \frac{\boldsymbol{Y}_k \otimes \boldsymbol{Y}_k}{\boldsymbol{Y}_k \cdot \boldsymbol{S}_k} - \frac{(\boldsymbol{H}_k \cdot \boldsymbol{S}_k) \otimes (\boldsymbol{H}_k \cdot \boldsymbol{S}_k)}{\boldsymbol{S}_k \cdot \boldsymbol{H}_k \cdot \boldsymbol{S}_k}$$

with $\boldsymbol{Y}_k = \nabla F(\boldsymbol{X}_{k+1}) - \nabla F(\boldsymbol{X}_k)$. The distance of descent is computed using Armijo's rule, where $\alpha_k = (\frac{1}{2})^m$ and $m$ is the smallest integer such that the relationship

$$F(\boldsymbol{X}_k + \alpha_k \boldsymbol{S}_k) \le F(\boldsymbol{X}_k) + \sigma\alpha_k \nabla F(\boldsymbol{X}_k) \cdot \boldsymbol{S}_k$$

with $\sigma$ being the sufficient descent criterion, which must be chosen between 0 and $\frac{1}{2}$ (usually set to $10^{-4}$).

### D. Initial Solution

In most cases, the optimization method described will yield a solution, but in the case of a highly nonlinear cost function such as the one in hand, the minimum found is usually a local one. One way to circumvent this difficulty is to proceed with many optimizations, starting from various initial guesses and selecting the lowest minimum as the optimal solution. Whereas this approach could be unaffordable if no clue were available about the optimal solution, it can be implemented relatively cheaply in the context of curve approximation, where many good initial guesses can be constructed.

Specifically, a set of initial solutions is constructed by discretizing the target curve using a fixed number of points and by varying the concentration of points along the curve. Basically, points are placed closer together in regions of high curvature, and a shifting constant is introduced to construct various concentration laws. For target curves of continuity lower than $C^2$, curvature is approximated using centered differencing. The concentration law is evaluated using

$$\mathcal{F}(u) = \frac{1}{K}\int_0^1 [C(v) + D]\, \mathrm{d}v$$

where $C(v)$ is the true or approximated curvature of the target curve, $D$ the shifting constant, and $K$ a normalization factor such that $\mathcal{F}(u) = 1$.

As the shifting constant increases, the concentration law becomes almost uniform. In practice, sets of 8–10 initial solutions are constructed by varying $D$, typically between 1.0 and 10, and then using each initial solution as the starting point for the optimization process. Figure 1 shows the final approximation error for a run where $D$ took the values $\{0.5, 1.0, 2.5, 3.0, 3.5, 4.5, 5.0, 6.0, 7.0\}$. The target curve for this problem is a NACA 2412 airfoil and 9 control points are used for the approximation, which leads to a 21-parameter optimization problem (the two endpoints are fixed). Initial weights are all set to 1.0.

Figure 1 vividly illustrates the high degree of nonlinearity of the problem and the existence of local optimas, where small variations in the initial solution lead to different optimal solutions, as expressed, for example, by the steep variation in final error for $D = 4.5$ and $D = 5.0$. Note, however, that, as discussed in the next section, both of these initial solutions are accurate enough in the context of geometrical representation of airfoils.

## III. Optimized NURBS Airfoils

Different airfoils have been approximated using the optimized NURBS representation to determine the number of control points that could represent any wing section to a given accuracy. The following airfoils are representative of our tests: 1) NACA 2412, defined by a 160-point spline; 2) RAE 2822, defined by a 130-point spline; 3) Bombardier–Canadair (BC) supercritical airfoil defined with 160 points; 4) Boeing A4, defined by an 80-point spline; and 5) Boeing A8, defined with 190 points.[4]

Figure 2 illustrates the evolution of $\varepsilon_{\max}$ as the number of control points of the approximation curve is increased. The target curve is the NACA 2412 airfoil. As can be observed, the increase in precision of the approximation is very regular when eight or more control points are used. The precision required for a good approximation has been studied in Ref. 5. A precision of $8 \times 10^{-5}$ for an airfoil of chord one has been found sufficient based on the sensitivity of the flow solver to the geometric definition. In the case of the NACA 2412 airfoil, the required precision of $8 \times 10^{-5}$ is obtained with only nine control points.

Extensive experiments[5] involving numerous types of wing profiles have shown that the required level of precision can almost always be reached with 13 control points or fewer. As an example, the approximation errors for a 13-control-point NURBS approximation are shown in Table 1 for selected airfoils. These results show that, no matter how different these curves may be, it should always be possible to approximate them using 13 or fewer control points.

These numbers have to be compared with the number of points needed to represent an airfoil discretely with the same precision,

**Table 1 Error for 13-control-point approximation**

| Profile | $\epsilon_{\max}$ error |
|---|---|
| NACA 2412 | $2.6 \times 10^{-5}$ |
| RAE 2822 | $2.3 \times 10^{-5}$ |
| BC | $7.9 \times 10^{-5}$ |
| Boeing A4 | $8.1 \times 10^{-5}$ |
| Boeing A8 | $8.2 \times 10^{-5}$ |

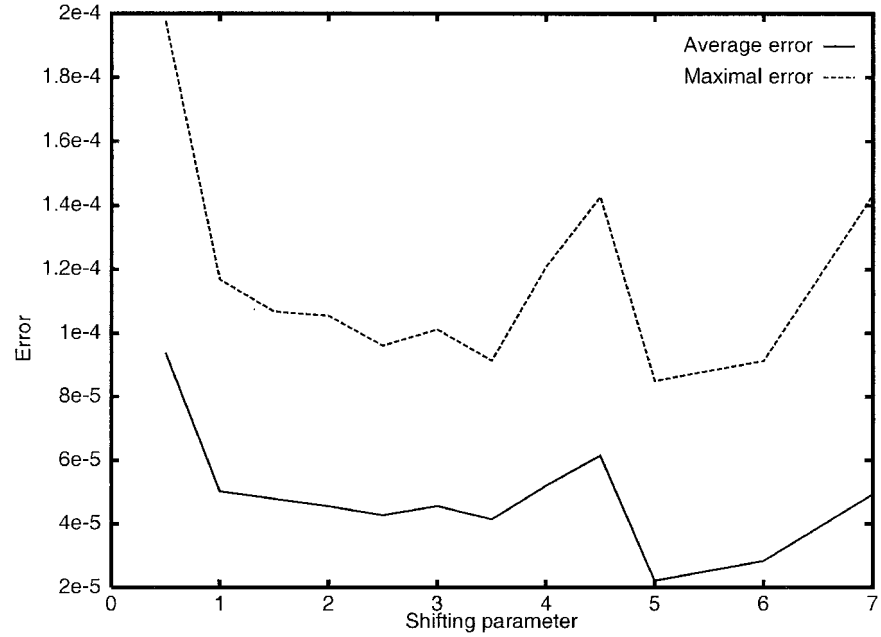


**Fig. 1 Optimal approximation error for various shifting constant values.**

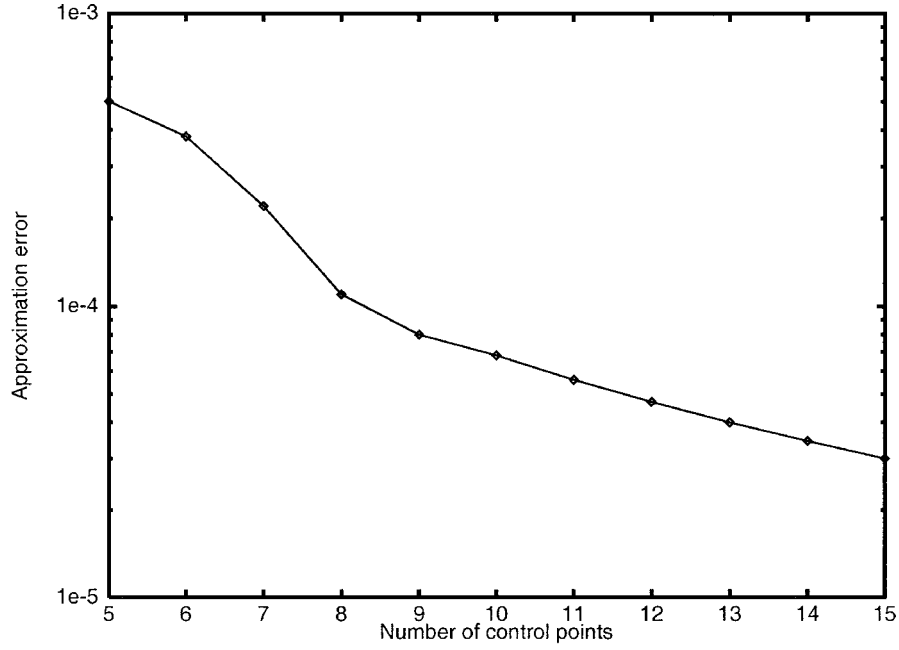


**Fig. 2 Precision of approximation as number of control points increases.**

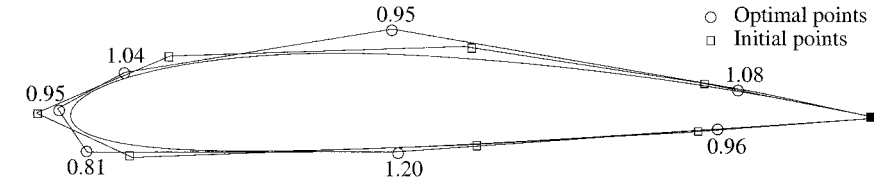


**a) NACA 2412 approximation (9 point)**

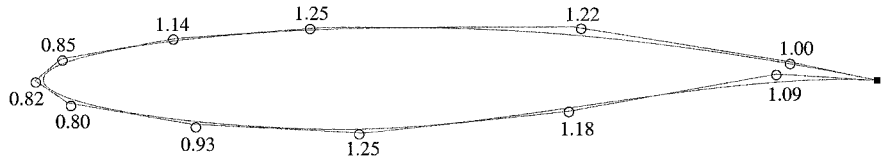


**b) RAE 2822 approximation (13 point)**

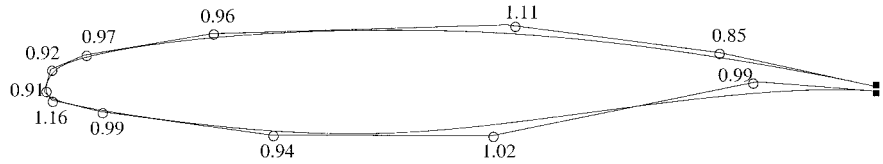


**c) BC approximation (13 point)**

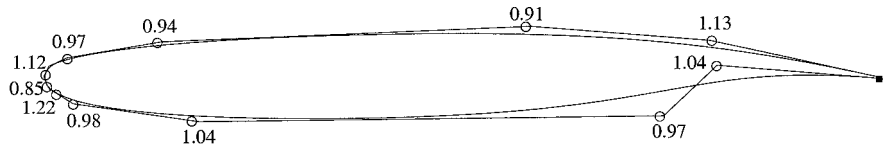


**d) Boeing A4 approximation (13 point)**

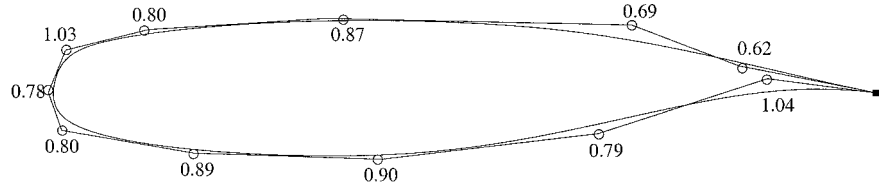


**e) Boeing A8 approximation (13 point)**

**Fig. 3 Optimized NURBS approximation of various wing profiles.**

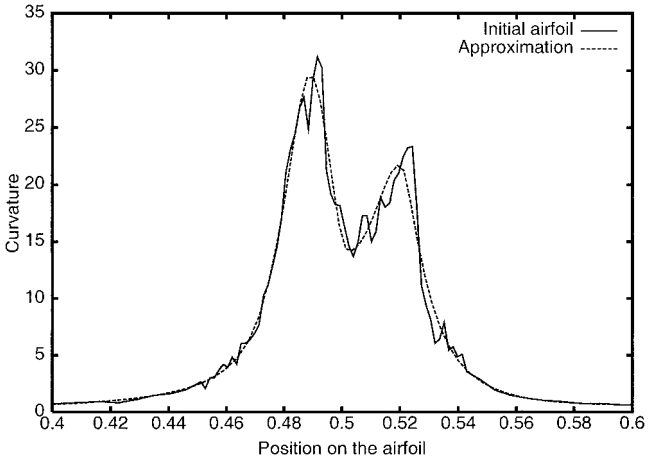


**Fig. 4 Curvature of Boeing A8 profile and of its approximation near leading edge.**

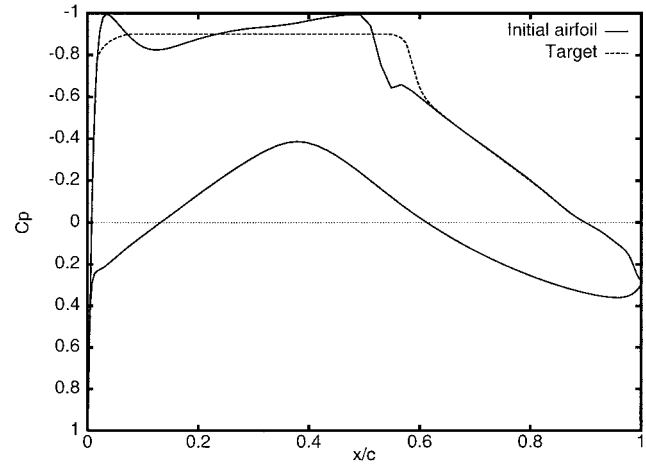


$M = 0.735$, $C_L = 0.6$ and $Re = 10^7$

**Fig. 5 Target pressure for aerodynamic optimization of BC profile.**

which can be shown to be of the order of 150 if the discrete points are distributed in a reasonable manner. The NURBS approximation method thus offers excellent control over the precision of the resulting curve, while reducing by an order of magnitude the amount of data used for representation using discrete points.

Figure 3 displays the approximation of the selected airfoils with their optimized control point positions and weights. Figure 3 illustrates that the range of airfoils that can be represented with this method is very wide. This point is very important because the airfoil will later have to be optimized to improve its aerodynamic characteristics, and the geometric representation must provide enough freedom to enable the optimizer to converge toward a better airfoil.

For the optimization, the control points positions and weights are freely varied by the optimizer, and although the weigths are modified by the optimization process, experience has shown that they are only varied by small amounts (no more than 20%) around their initial

value of one. For this application, no special constraints need to be imposed on the weights, neither for theoretical nor practical reasons.

The proposed NURBS approximation method also has the ability to filter noise in the representation, mainly because of the small number of control points needed. Noise appears as small, high-frequency fluctuations in the curvature of the airfoil, usually observed when control points are close together in regions of high curvature. Figure 4 illustrates the curvature of the Boeing A8 airfoil and the curvature of its optimized NURBS approximation. The proposed NURBS approximation method significantly reduces noise in the geometric representation. Of course, this noise reduction can only be accomplished as a tradeoff against the precision of the approximation. In fact, the precision of the 13-control-point approximation of the Boeing A8 airfoil is $9.2 \times 10^{-5}$, which is slightly above the tolerance goal for this application. A better precision could be obtained by including a few more control points, but this would inevitably introduce more noise.

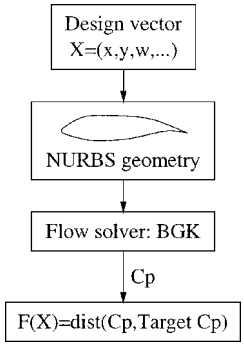


**Fig. 6 Objective function computation.**

## IV. Application to Aerodynamic Optimization

As shown in the preceding section, the proposed geometrical representation for airfoils results in few design parameters, which significantly reduces the risk of noise. The method is, thus, expected to make the aerodynamic optimization process significantly easier. This section will present examples of such aerodynamic optimizations in two and three dimensions.

Wing design optimization can be achieved by several means. One is the direct method, the goal of which is to optimize the global characteristics of the profile (for example, the lift-to-drag ratio). This method is quite difficult to implement because it is not easy to control the shape modifications. Successful results have recently been

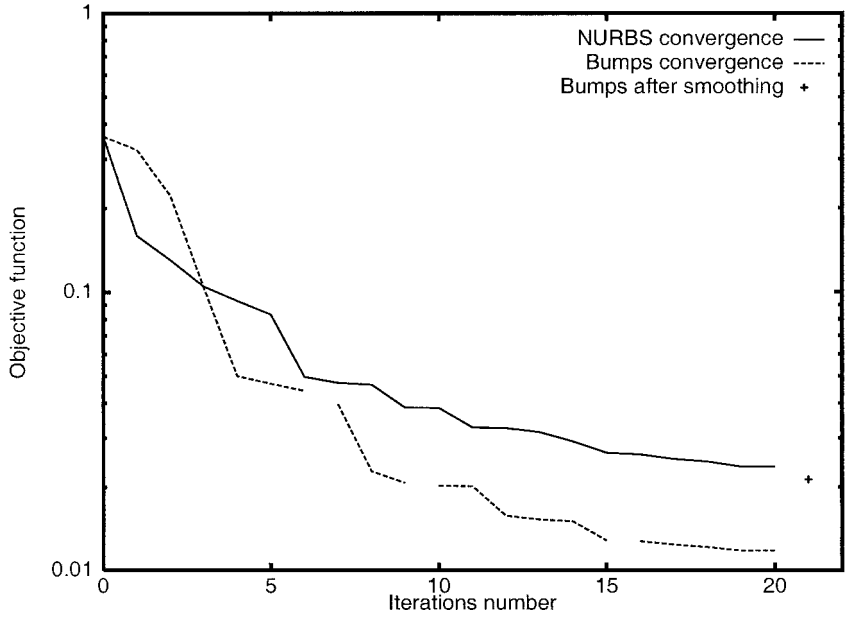


**Fig. 7 Optimization convergence (two-dimensional case).**

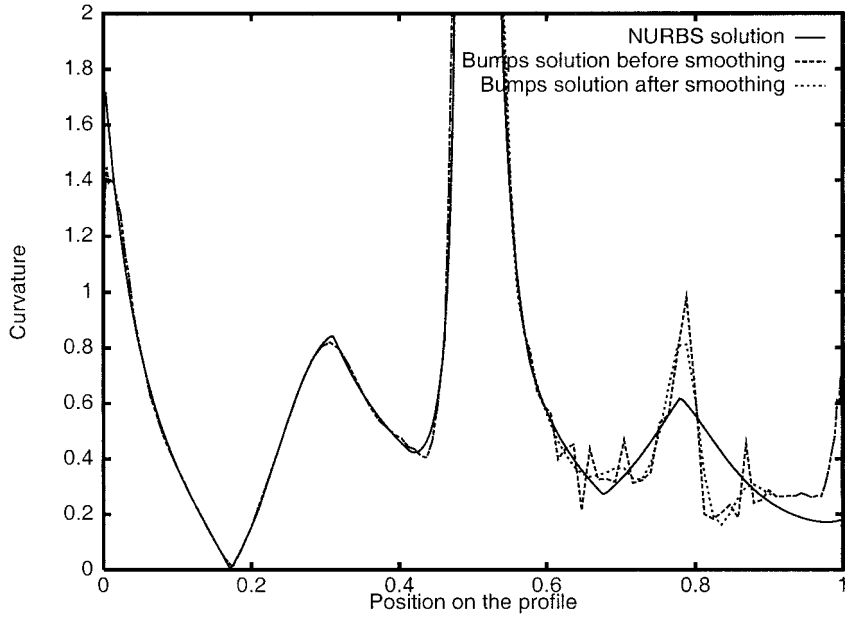


**Fig. 8 Curvature of optimized profiles.**

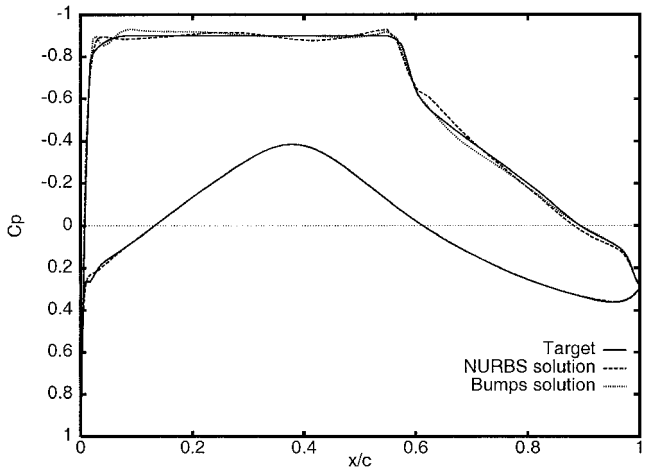


**Fig. 9 $C_p$ of optimized profiles.**

reported in Ref. 6 using Hicks–Henne shape functions as design variables. Other examples of such optimizations can be found in Refs. 7–10. A different approach, called the indirect method, consists of setting a target pressure coefficient distribution and searching for an airfoil having such a pressure distribution. This indirect method is still widely used by aerodynamic designers in the industry and, for an experienced designer, results easily in realistic airfoils. In fact, this method is often used even though the definition of the ideal pressure distribution is, by itself, a tricky problem, as reported in Refs. 11–17. The examples of aerodynamic optimization presented in this section are based on the indirect method.

### A. Two-Dimensional Optimization

The indirect method consists of defining an objective for aerodynamic design in terms of a pressure coefficient $C_p$ distribution on the airfoil section. Figure 5 displays the initial $C_p$ curve, computed for the BC profile at Mach = 0.735 (Fig. 3c) with the flow solver Bauer–Garabedian–Korn (BGK)[18,19] solving the potential equations coupled with a boundary-layer analysis. The target pressure distribution

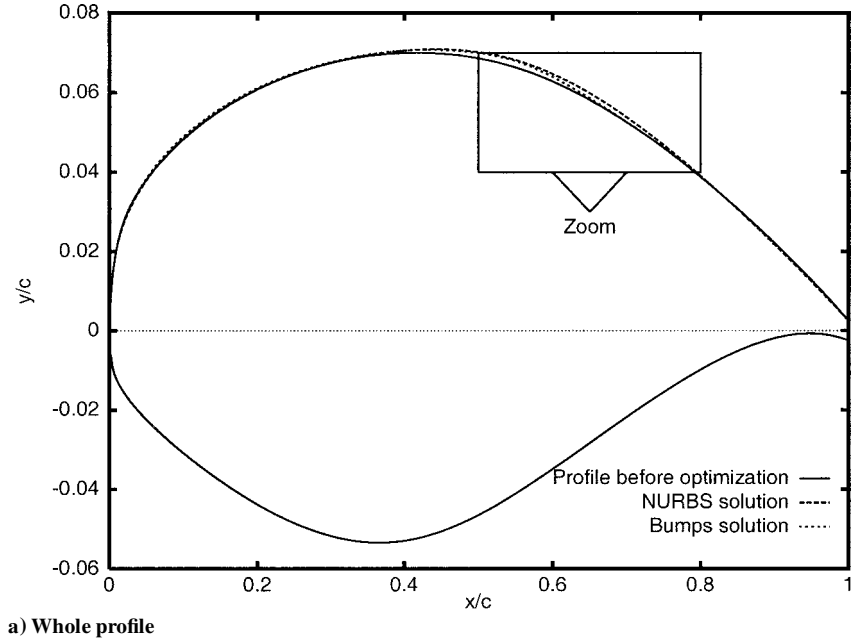


**a) Whole profile**

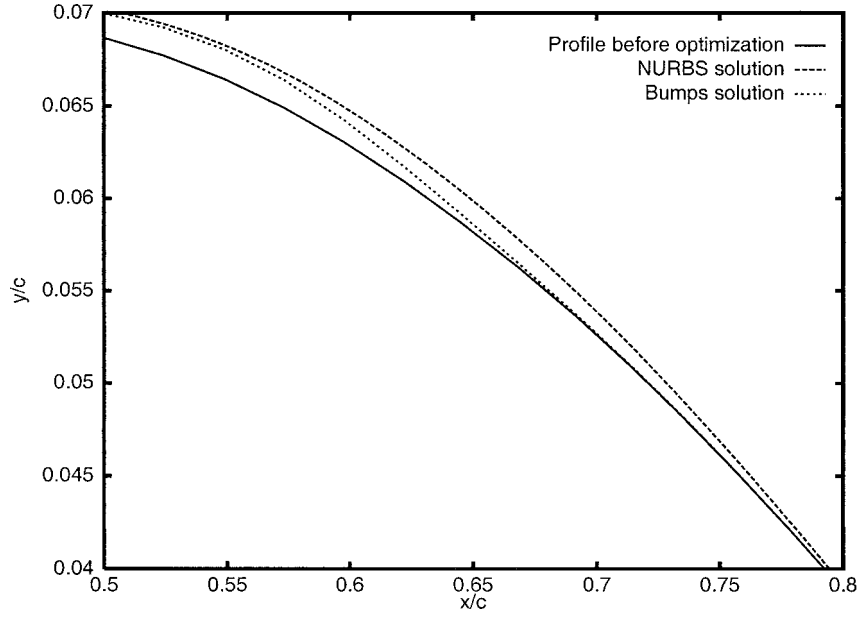


**b) Magnification of upper surface**

**Fig. 10 Profiles before and after optimization.**

that has been specified to improve the aerodynamic characteristics of the airfoil is also shown in Fig. 5.

The global aerodynamic optimization process is based on the quasi-Newton BFGS method, minimizing an objective function computed as illustrated in Fig. 6. Derivatives of the objective function are computed using finite differences. The objective function computes the distance between the current airfoil pressure distribution computed using a BGK flow solver and the target pressure distribution. A vector of design parameters contains the NURBS control point coordinates as well as their weights. In this example, only the upper surface of the airfoil is to be modified, so that only the $y$ coordinates and the weights of selected control points are modified, resulting in a total of 11 design variables.

For comparison, optimization has also been conducted in parallel using a 160-point representation augmented with airfoil shape functions, introduced by Hicks and Vanderplaats[20] and applied by Hicks and Henne.[21] The number of shape functions (also called bumps) has been limited to 11 to keep the number of design parameters in the two optimizations equal.

The convergence of the optimization process is presented in Fig. 7. At first glance, it could be thought that the bump method performs better than the NURBS method because it converges more rapidly. However, two circumstances have to be taken into account. First, each interruption in the bump method convergence curve corresponds to a human intervention to restart the optimizer with new bump characteristics. Without these interventions, a realistic solution is difficult to obtain. The need for human intervention makes the design process considerably more complicated. Second, the bump method introduces significant noise in the airfoil definition, so that the final airfoil geometric definition must be smoothed at the end of the optimization. The smoothing operation is not only time consuming, but it also significantly reduces the overall optimization efficiency. This is illustrated in Fig. 7, which shows that the objective function obtained with the bump method after smoothing approaches the NURBS objective function. The curvature of the optimized profiles is shown in Fig. 8. Significant noise is observed on the airfoil extrados in the region of the shock for the bump method solution, and noise is still present after the smoothing process. By

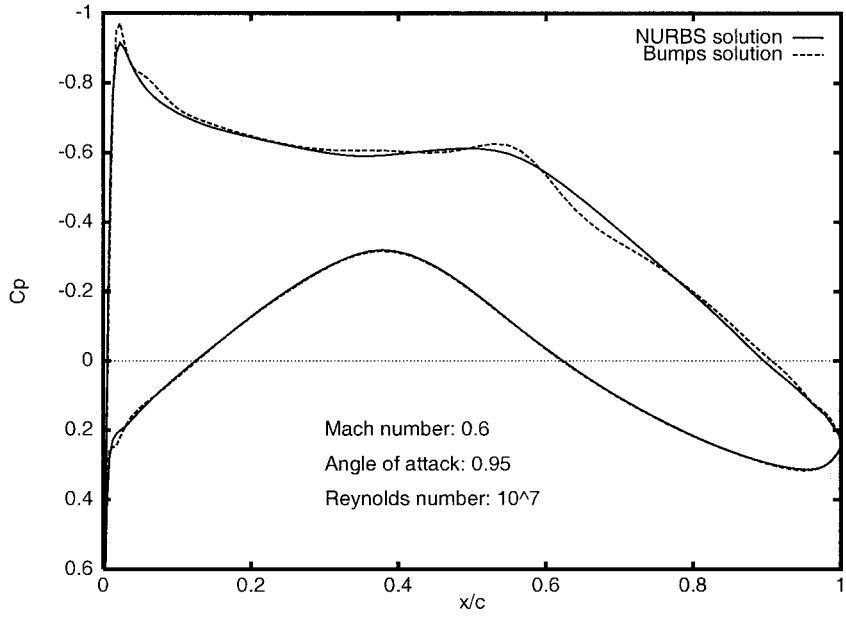


**a) $C_p$ of optimized profiles for Mach = 0.6**

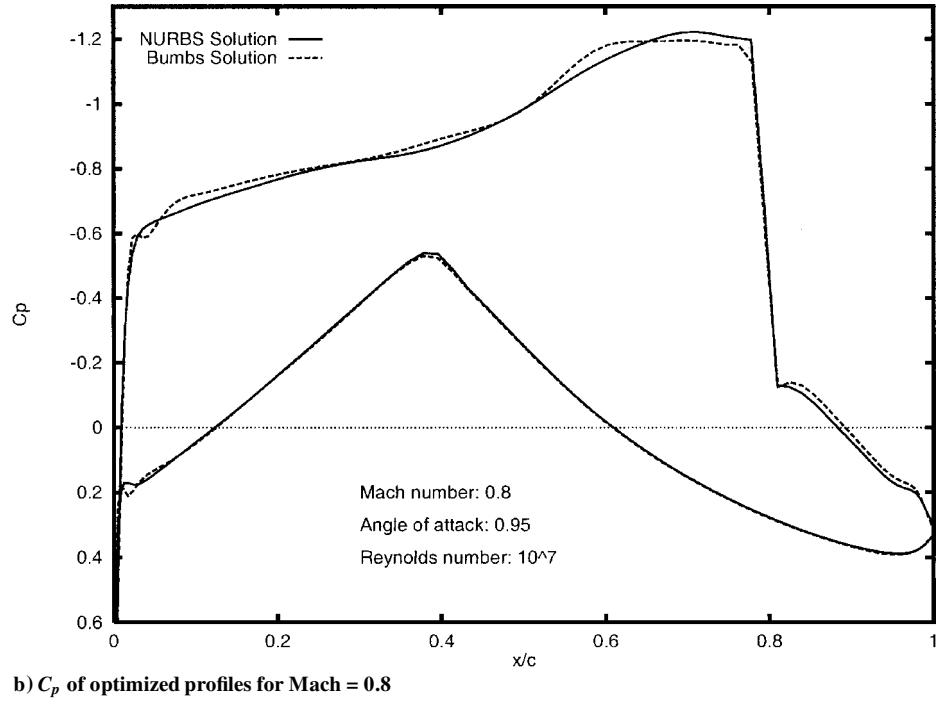


**b) $C_p$ of optimized profiles for Mach = 0.8**

**Fig. 11 Off-design performance results.**

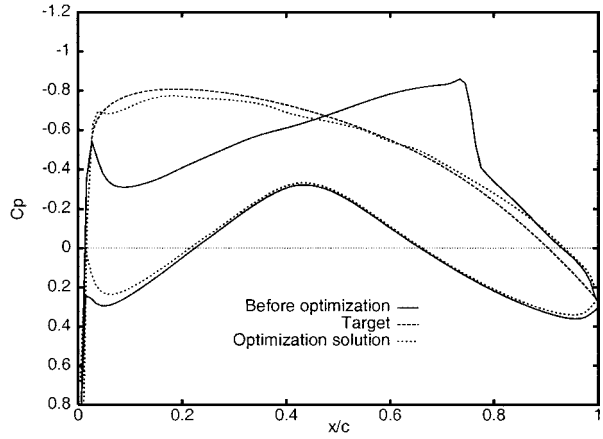


a) First section (wing–body junction)

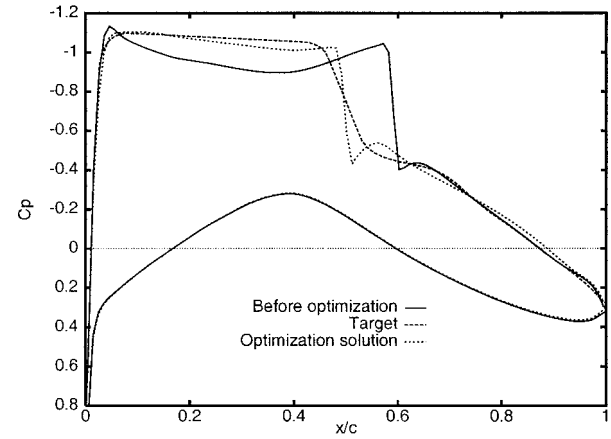


c) Fifth section

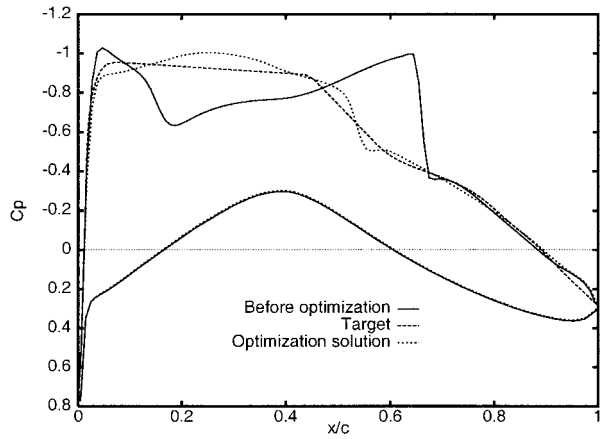


b) Third section

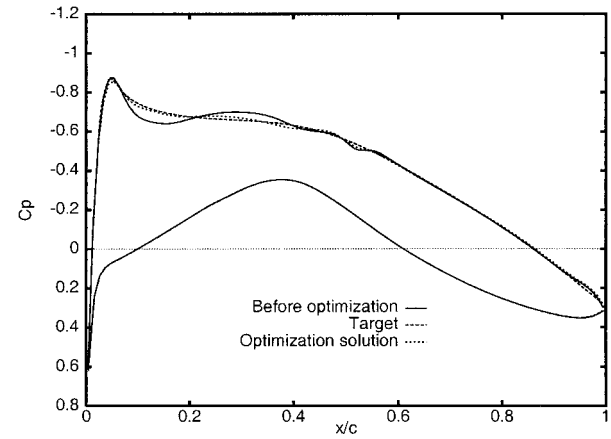


d) Seventh section (wing tip)

**Fig. 12 Modification of $C_p$ curves during optimization.**

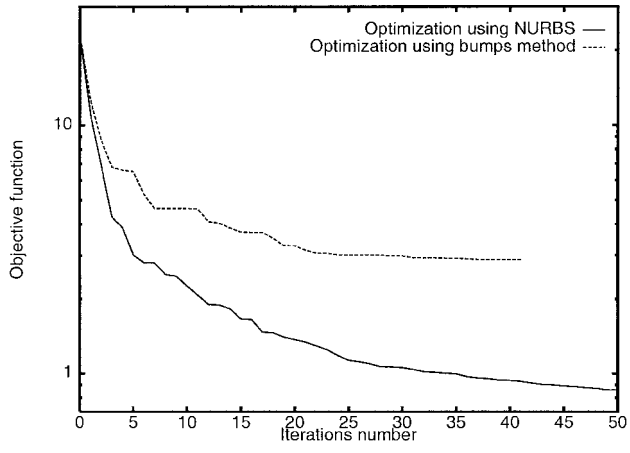


**Fig. 13 Optimization convergence (three-dimensional case).**

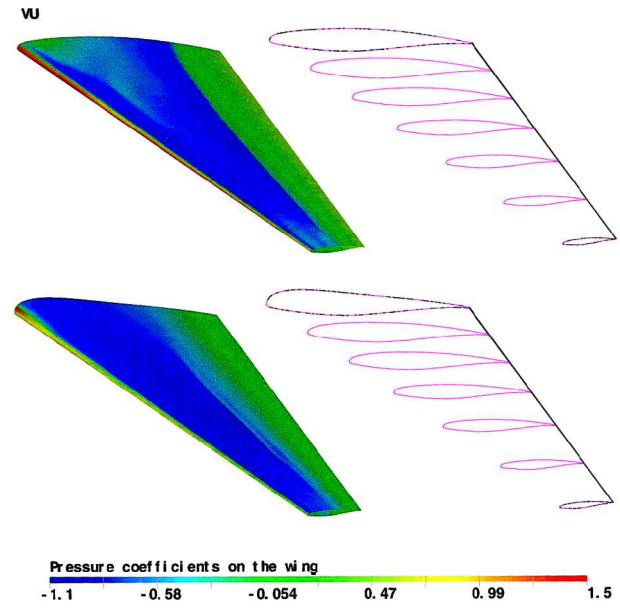


**Fig. 14 Three-dimensional wing optimization: pressure and wing section profiles before (top) and after (bottom) optimization.**

contrast, the NURBS method has led, without any human intervention, to a satisfactory solution that is free of noise.

The pressure distributions obtained are shown in Fig. 9. Note that the NURBS optimized profile leads to a much smoother flow close to the leading edge of the airfoil.

Figure 10 depicts the airfoil profile before and after optimization, as well as a magnification of a part of the upper surface. On the one hand, the small magnitude of the profile modification during the optimization process indicates the sensitivity of the aerodynamic design problem. On the other hand, it can be seen that both methods have led to rather different solutions in the shock region, which has been magnified in Fig. 10b. In this close-up, it can be observed that there is a jump in the bump method solution. This jump is an artificial way for the optimizer to impose the position of the shock, but this leads to a loss of smoothness for the airfoil representation, which can also be seen in Fig. 8. This lack of smoothness can damage the performance of the airfoil under off-design conditions. This is confirmed in Fig. 11, which shows the pressure distribution on both solution profiles for Mach numbers equal to 0.6 and 0.8, compared to 0.735 for the design point. Indeed, in the bump method solution, the pressure distribution at the location of the break is not smooth, whereas in the NURBS method solution there is a good degree of smoothness. This illustrates that the NURBS solution leads to a

more realistic airfoil because the geometric representation has better built-in control of the smoothness of the airfoil.

This example shows the two significant advantages of our method for aerodynamic optimization: It makes possible a more rapid and a more automatic design process, and it naturally constrains the airfoil to have good smoothness properties.

### B. Three-Dimensional Optimization

The same method is now applied to optimize a three-dimensional wing. The wing is defined by seven airfoil profiles with a linear interpolation in the spanwise direction. Each section is defined by a 13-control-point NURBS, and 11 parameters are selected for the optimization among the control point coordinates and weights. As a consequence, the complete problem contains 77 design variables.

As in the preceding example, the objective function is based on a target pressure distribution set at each of the seven sections to improve the wing's performance. The pressure distribution is computed with the small perturbation flow solver KTRAN for a Mach number equal to 0.8. Initial and final $C_p$ curves, as well as target pressure distributions that have been used for optimization, are displayed in Fig. 12. The target $C_p$ distribution was chosen such that the shock at the wing root is eliminated and the shock at the outboard stations is moved closer to the leading edge of the wing.

The summary of the convergence is depicted in Fig. 13. As shown in Fig. 13, when the NURBS representation for profiles is used, the optimization procedure runs without any problem, whereas no satisfactory solution has been obtained with the bump method. Indeed, the three-dimensional flow solver is very sensitive to noise in the definition of its geometry so that it is very difficult to make the bump method converge.

The effectiveness of the method is also emphasized in Fig. 14, in which the section profiles and the pressure before and after optimization on the upper surface of the wing are compared. As can be seen, the shock strength has been significantly reduced owing to the modification of the seven airfoil profiles. Of course, the objective pressure distribution was not reached exactly. However, the improvement in the wing's aerodynamic performance is very significant. Furthermore, the wing geometry remained very smooth during the optimization owing to its NURBS definition and to the small number of design variables. The modification of the airfoil profile at the wing root is the most significant of these. Note that use of the bump method cannot result in such a significant shape modification.

This example of aerodynamic optimization points up the efficiency of the NURBS method for geometric representation. Owing to the preliminary optimization of the number of design parameters, (i.e., the number of control points), an accurate definition of the complete wing has been obtained with very few design variables. This results in a rapid optimization procedure and a noiseless solution. In the case of the bump method, achieving equivalent accuracy would require a greater number of parameters, which would inevitably introduce noise.

## V. Conclusions

In this work, NURBS have been shown to constitute a very appropriate method for the geometric representation for wing design optimization because of their geometric properties. In particular, owing to an optimization process, NURBS have been shown to be capable of accurately representing a large family of airfoils with 13 or fewer control points. This method has various advantages: First, it minimizes the number of variables involved in the process of wing section design. Second, it constrains the airfoil to a natural smoothness. Third, a NURBS representation with 13 control points can be used for design optimization without reducing the range of available airfoils.

When applied to aerodynamic optimization, the method is found to be very powerful. Realistic solutions are computed with few iterations owing to the small number of design variables and to the smoothness of the geometry, which improves the convergence of the optimization process.

## References

[1]Samareh, J., "Status and Future of Geometry Modeling and Grid Generation for Design and Optimization," *Journal of Aircraft*, Vol. 36, No. 1, 1999, pp. 97–104.

[2]Piegl, L., and Tiller, W., *The NURBS Book*, Springer, Berlin, 1995, pp. 117–124.

[3]Lépine, J., Guibault, F., and Trépanier, J.-Y., "Optimization of a Curve Approximation Based on Nurbs Interpolation," *Curves and Surface Design: Saint-Malo 1999*, edited by P. J. Laurent, P. Sablonnière, and L. L. Schumaker, Vanderbilt Univ. Press, Nashville, TN, 1999.

[4]Jones, D. J., and Nishimura, Y., "A Selection of Experimental Test Cases for the Validation of CFD Codes," AR 303, AGARD, Aug. 1994.

[5]Trépanier, J.-Y., Lépine, J., and Pépin, F., "An Optimized Geometric Representation for Wing Profile Using NURBS," *CASI Journal*, Vol. 46, No. 1, 2000, pp. 12–19.

[6]Reuther, J., Jameson, A., Alonso, J., Rimlinger, M., and Saunders, D., "Constrained Multipoint Aerodynamic Shape Optimization Using an Adjoint Formulation and Parallel Computers (Parts 1 and 2)," *Journal of Aircraft*, Vol. 36, No. 1, 1999, pp. 51–74.

[7]Burgreen, G., and Baysal, O., "Aerodynamic Shape Optimization Preconditioned Conjugate Gradient Methods," *AIAA Journal*, Vol. 32, No. 11, 1994, pp. 2145–2152.

[8]Burgreen, G., Baysal, O., and Eleshaky, M., "Improving the Efficiency of Aerodynamic Shape Optimization," *AIAA Journal*, Vol. 32, No. 1, 1994, pp. 69–76.

[9]Sadrehaghighi, I., Smith, R. E., and Tiwari, S. N., "Grid Sensitivity and Aerodynamic Optimization of Generic Airfoils," *Journal of Aircraft*, Vol. 32, No. 6, 1995, p. 1234.

[10]Zhu, Z. W., and Chan, Y. Y., "An Efficient Optimization Method for Aerodynamic Designs—Geometric Genetic Algorithm," *Proceedings of the 6th Annual Conference of the CFD Society of Canada*, edited by E. Fournier, Defence Research Establishment Valcartier, Courcelette, QC, Canada, 1998, pp. II-9–II-14.

[11]Obayashi, S., and Oyama, A., "Three-Dimensional Aerodynamic Optimization with Genetic Algorithm," *Proceedings of the Third ECCOMAS CFD Conference*, Wiley, Chichester, England, U.K., 1996, pp. 420–424.

[12]Obayashi, S., and Takanashi, S., "Genetic Optimization of Target Pressure Distributions for Inverse Design Methods," *AIAA Journal*, Vol. 34, No. 5, 1996, pp. 881–886.

[13]Obayashi, S., Takanashi, S., and Fejtek, I., "Transonic Wing Design by Inverse Optimization Using MOGA," *Proceedings of the 6th Annual Conference of the CFD Society of Canada*, edited by E. Fournier, Defence Research Establishment Valcartier, Courcelette, QC, Canada, 1998, pp. II-41–II-46.

[14]Obayashi, S., and Tsukahara, T., "Comparison of Optimization Algorithms for Aerodynamic Shape Design," *AIAA Journal*, Vol. 35, No. 8, 1997, pp. 1413, 1414.

[15]Selig, M., and Maughmer, M., "Generalized Multipoint Inverse Airfoil Design," *AIAA Journal*, Vol. 30, No. 11, 1992, pp. 2618–2625.

[16]Selig, M., and Maughmer, M., "Multipoint Inverse Airfoil Design Method Based on Conformal Mapping," *AIAA Journal*, Vol. 30, No. 5, 1992, pp. 1162–1170.

[17]Vicini, A., and Quagliarella, D., "Inverse and Direct Airfoil Design Using a Multiobjective Genetic Algorithm," *AIAA Journal*, Vol. 35, No. 9, 1997, pp. 1499–1505.

[18]Bauer, F., Garabedian, P., and Korn, D., *Supercritical Wing Sections*, No. 66, Lecture Notes in Economics and Mathematical Systems, Springer-Verlag, Berlin, 1972.

[19]Bauer, F., Garabedian, P., Korn, D., and Jameson, A., *Supercritical Wing Sections II*, No. 108, Lecture Notes in Economics and Mathematical Systems, Springer-Verlag, Berlin, 1975.

[20]Hicks, R. M., and Vanderplaats, G. N., "Application of Numerical Optimization to the Design of Supercritical Airfoils with Drag Creep," Society of Automotive Engineers, Paper, No. 0440, Vol. 77, 1977.

[21]Hicks, R. M., and Henne, P. A., "Wing Design by Numerical Optimization," *Journal of Aircraft*, Vol. 15, No. 7, 1978, pp. 407–412.

A. Plotkin
*Associate Editor*